OMAE2017-62540

WAVE DRIFT FORCES AND LOW FREQUENCY DAMPING ON THE EXWAVE FPSO

Nuno Fonseca
SINTEF Ocean
Trondheim, Norway
nuno.fonseca@sintef.no

Carl Trygve Stansberg
Ctstansberg Marinteknikk
Trondheim, Norway
ctstansberg.marinteknikk@gmail.com

ABSTRACT

A method is followed in the present analysis to estimate realistic surge and sway wave drift force coefficients for the Exwave FPSO. Model test data is used to identify the difference frequency wave exciting force coefficients based on a second order signal analysis technique. First, the slowly varying excitation is estimated from the relationship between the incoming wave and the low frequency motion using a linear oscillator. Then, the full QTF of the difference frequency wave exciting forces is defined from the relationship between the incoming waves and the second order force response. The process identifies also the linearized low frequency damping.

The paper presents results from a few cases selected from the Exwave JIP test matrix. Empirical mean wave drift coefficients are compared to potential flow predictions. It is shown that the latter underestimate the wave drift forces, especially at the lower frequency range where severe seastates have most of the energy. The sources for the discrepancies are discussed..

1 INTRODUCTION

There has been cases where conventional calculation procedures based on potential flow codes and Newman's approximation tend to under-predict wave drift forces on FPSOs, especially in severe seastates. The reasons might be higher than second order potential flow effects, QTF off diagonal terms deviating from Newman's approximation, viscous effects, or other phenomenon not taken into account by the linear radiation/diffraction theory (QTF - quadratic transfer function of exciting forces). Conditions with current add complexity and increase discrepancies, see e.g. Hermundstad et al. (2016). Since, at least for the observed cases (although in principle not always true), the tendency is to under predict wave drift forces, the consequence is that predicted slow drift motions may be under-estimated, as well

as maximum mooring line tensions (compared to model test data, for example).

Aksnes et al. (2014, 2015) compare measured and calculated slow drift motions and mooring line tensions for FPSOs in the Norwegian fields. Wave drift forces are based on Newman's approximation. The conclusion for these two cases is that potential flow wave drift force coefficients need to be increased for good agreement of predictions with test data. Aksnes et al. (2015) presented results for turret moored FPSO, with tanker type of hull form, including a small bulb at the bow, a flared bow above the waterline and vertical sides below the waterline. The overall length is around 270 m. The test case corresponds to a seastate with significant wave height and peak period of 15.6 m and 16 s and no current, neither wind. The mooring system is composed of wire and chain catenaries.

The authors (Aksnes et al.) compare time domain simulations with model test data and show that predictions based on linear potential flow wave drift coefficients underestimate the surge slow drift motions and the extreme mooring line tensions. Correction of the wave drift coefficients based empirical values identified from the model test data, improves the predictions as compared to test data. The correction consists on increasing the drift coefficients at the low frequency range. Similar tendencies have been observed for other FPSOs, however the observed cases correspond to vessels with lengths between 240 and 260 m (Lpp) and displacements between 130 and 180 thousand tonnes, therefore representative of medium size FPSOs. One realizes that more work is needed to clarify how important are these observations for the broader industry needs.

Therefore, one of the main objectives of the Exwave JIP is to address the need to improve today's procedures to calculate wave drift forces induced by severe seastates on floating structures, including current (Fonseca et al. 2016). Fonseca et al. (2017) present a summary of the project results

and progress until the end of 2016. More specifically regarding FPSOs, the aims are: (a) to understand the reasons why linear diffraction theory appears to fail for some cases and (b) to improve present calculation procedures based on physical interpretation of the involved phenomena.

The problem is tackled with a combination of dedicated model tests and numerical studies. Two structures are selected as case studies: a semi-submersible representative of a classical four column drilling rig and a FPSO hull. The present paper deals with the FPSO, while another publication presents and discusses results for the Semi (Fonseca and Stansberg, 2017).

An important part of the work program consists on performing model tests, post-processing of the data and interpretation of results. The paper presents the Exwave FPSO experimental program and the analysis performed to identify wave drift force coefficients from the test data. The procedure uses the irregular wave elevation and the low frequency (LF) measured motions time histories, together with a second order signal analysis technique, to identify the difference frequency wave exciting quadratic transfer function (QTF).

The empirical wave drift coefficients are compared with potential flow predictions and with results derived from periodic wave tests. The surge low frequency damping is estimated and discussed as well.

2 MODEL TESTS

Model tests were performed at the Ocean Basin Facility at MARINTEK during March 2016 with a 1:70 scaled model of the Exwave FPSO (FPSO: Floating, Production, Storage and Offloading vessel). The vessel was designed for turret moored operation and can be considered as representative of a FPSO modern hull design. Figure 1 shows a photo of the model, while Table 1 presents the platform main particulars.

The tests focused on the dynamic behaviour of the vessel in waves and current. The aim of the model test program was to obtain test data to: (a) identify the slowly varying wave drift forces and the related slow drift damping and (b) assess the quality of slow drift motions numerical predictions. The focus is on the horizontal low frequency motions induced by severe seastates. The wave-current interaction effects on the wave drift forces are also addressed.

The tests were performed at 3 m water depth (210 m full scale), which may be considered as deep water conditions for most of the wave frequency range of interest (for frequencies below around 0.05 Hz there might be some bottom effect on the wave drift forces). The vessel was moored with a soft horizontal mooring system with (almost) linear restoring forces in surge and sway. The system is composed of 4 thin lines with horizontal angular separation of 45 degrees. Two lines attach at the model bow and two at the stern, with the other ends at the Ocean Basin sides. Each line includes a system of springs with designed stiffness, Decay tests identified the following surge natural periods:

Uc = 0:   Tn = 169.6 s
Uc = 0.97 m/s: Tn = 168.0 s

Parameters such as the wave height and current velocity are changed systematically with the objective of characterizing their influence on the wave drift forces. Both regular and irregular wave conditions were used. Pull out and decay tests were performed as well.

Figure 1: EXWAVE FPSO 1:70 scaled model.

Table 1: EXWAVE FPSO main properties.

Parameter	Unit	Full scale
Length between perpendiculars	[m]	244.0
Beam	[m]	48.0
Depth	[m]	26.6
Displacement	[t]	178365
Draught at midship	[m]	18.58

The measured responses from the tests in waves include: wave elevation, vessel motions, accelerations at the deck, relative motions, global horizontal mooring system forces and mooring line forces at the fairleads.

The measured signals from the periodic wave tests (periodic waves) are post-processed to identify their harmonic contents, namely the: mean value, 1st, 2nd and 3rd harmonic amplitudes and periods, and the response amplitude operator (RAO) and related relative phase angle. Some simple statistics are calculated as well.

The time records from the irregular wave tests are post-processed in terms of spectral analysis and statistical analysis. The analysis is carried out for: the signals as measured, low pass filtered signals and high pass filtered signals. The filtering frequency is 0.03 Hz full scale.

3 SECOND ORDER SIGNAL ANALYSIS

3.1 Modelling and estimation of slowly varying wave drift forces

Second-order slowly varying forces are usually modelled either by use of mean wave drift coefficients combined with Newman's approximation, or by full quadratic transfer functions (QTFs). Both approaches are in use in the industry today (se for example DNV GL, 2010). The first approach, using information from the mean drift coefficients in harmonic waves only (QTF main diagona), is clearly simpler and frequently preferred in engineering routine applications. Although the result is certainly a simplification with limitations, it has been a common view that the simplification can work reasonably well for horizontal motions of moored vessels in deep water.

In our present study, which is limited to slowly varying surge and sway in deep or almost deep water, we shall focus mainly on the wave drift coefficients. Thereby a main goal of the work is to estimate, from a system identification procedure, empirical drift coefficients from model test data in various sea states. Comparisons to numerical drift coefficients from standard potential flow predictions will also be made. Furthermore, we shall briefly address the limitations in the use of Newman's approximation. In principle, the identified drift coefficients can be used directly in the form of full QTFs, or they can be used to extract one difference frequency diagonal only to be used for generation of drift forces in the time domain through application of Newman's approximation. The text below clarifies further this aspect.

The estimation of empirical drift force coefficients or QTFs from experiments is not straightforward. The simplest way is to run a large number of regular (and bi-chromatic in case of QTFs) waves with various periods and steepness. An alternative and much more efficient but also complex procedure is to extract QTFs from tests in irregular waves, by use of cross-bi-spectral analysis between the incoming wave and resulting forces or motions. One implementation of such a procedure is described in Stansberg (1997), Pakozdi (2014), and some applications are presented in Stansberg (2001), Stansberg & Pakozdi (2009), Fonseca et al. (2016). Empirical drift coefficients, which we consider in the present work, can be derived from the empirical QTFs. Since we are aiming at coefficients that can be used to reproduce actual measured responses, we focus on an off-diagonal cross-section at a distance $\Delta f \approx 1/T_n$, where T_n is the natural period of the slowly varying motion. The low frequency motion results depend strongly on the excitation at this difference frequency.

Since, as in this case also, the measurements usually include slowly varying motions only and not direct force measurements, while we are aiming at force coefficients, one has to eliminate as far as possible the disturbance from the slow-drift dynamics. The procedure applied in the above references as well as in this study is to assume a linearized one degree of freedom (1 DOF) oscillator model for the dynamics. A deconvolution is run with an appropriate transfer function that is initially estimated from the slow-drift spectrum and then adjusted through iteration including repeated second-order simulations with the QTF. A linearized damping is then also obtained. Such a procedure has shown promising results through various experimental and numerical studies, see e.g. the above references. Still, one has to be aware of possible limitations due to the linearization of real nonlinear mooring stiffness and nonlinear damping (in the present case the stiffness is almost linear however). In addition, with off-diagonal variation in the QTF one must be careful in the distinction between dynamics and QTF variation; one should make use the information that is already available from decay tests on natural period and damping in still water and compare to the spectra.

3.2 Example

This Section presents an example of results from the cross bi-spectral analysis for a Torsethaugen long crested seastate with Hs = 7.7 m and Tp = 15 s. The FPSO heading is 0 degrees, which means head waves and there is no current. The test duration was 3.9 hours, full scale, and the initial 20 minutes were removed before the time signals were used for the cross bi-spectral analysis.

Figure 8 shows the estimated surge QTF of the difference frequency wave exciting forces. The bi-frequency plane axes are in Hz. The pink lines follows a diagonal with constant difference frequency of 0.0060 Hz, which corresponds to the surge natural frequency.

The quality of the identified QTF is assessed by comparing the measured low frequency motion with the same motion calculated using wave exciting forces reconstructed from the identified QTF. The comparison is done in terms of time histories and low frequency spectra. An example is presented in Figures 1 and 2 for the same seastate and vessel condition of the previous paragraph. The agreement between measured and reconstructed signals is good, which validates the QTF empirical estimation (under the assumption that the 1 DOF linear oscillator represents correctly the LF motion).
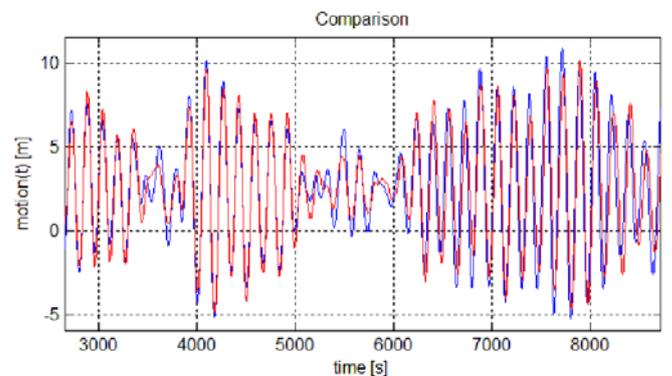

Figure 1: Comparison betw. measured slow drift surge motion (blue line) and reconstructed from the identified empirical QTF (red line).
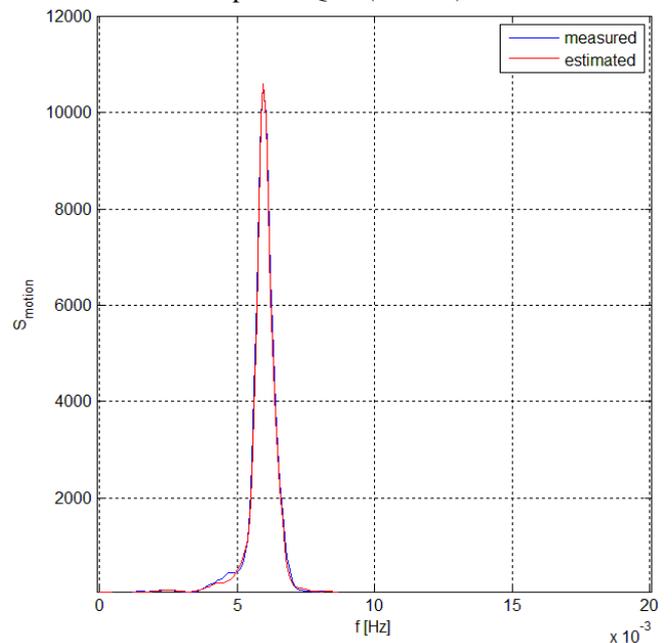

Figure 2: Spectra of low frequency surge motion. Comparison between exp. spectra (blue) and reconstructed spectra calculated from the identified QTF (red).

4 MEAN WAVE DRIFT FORCE COEFFICIENTS

4.1 Numerical model

Potential flow hydrodynamic coefficients, first order wave exciting forces and mean wave drift forces have been estimated by a 3D linear radiation-diffraction flat panel method (MULDIF, Hermundstad et al. 2016). The hull was modelled using 7598 panels, where the largest element diagonal is close to 3 m. Figure 3 presents the numerical model mesh.

The motions stiffness matrix includes mooring system linear restoring coefficients for the surge, sway and pitch modes. The latter is a very small value, compared to the hydrostatic stiffness. The natural periods estimated from the restoring coefficients and total system mass are (coupling between modes neglected):

Surge: Tn = 168.4 s
Heave: Tn = 11.3 s
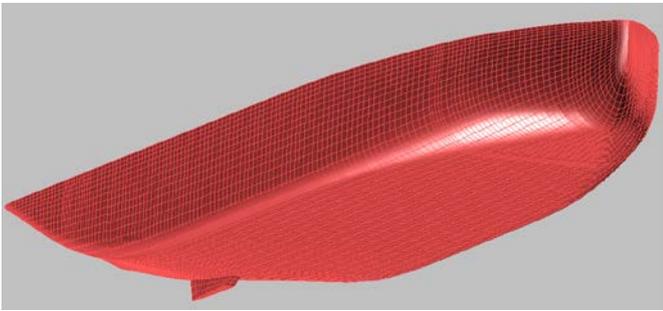Pitch;   Tn = 9.7 s

Figure 3: FPSO hull mesh for MULDIF hydrodynamic calculations.

4.2 Wave drift force coefficients identified from irregular wave tests

Although the cross bi-spectral analysis procedure identifies the full QTF, the present Section compares results from one diagonal only with mean wave drift coefficients from a potential flow code (MULDIF).

The surge and sway mean wave drift force coefficients, corresponding to the zero difference frequency ($df = f_1 - f_2$) components of the quadratic transfer functions (QTF[f_1, f_2]), were extracted from the empirically estimated QTFs. In fact, an approximation is applied, instead of extracting directly the zero Δf coefficients from the QTF. The slow drift motion spectra have more energy close to the natural frequency of the vessel plus mooring system (f_n) and therefore the estimations are considered more accurate for difference frequencies around fn. For this reason, the procedure consists on extracting a diagonal with Δf between $\Delta f = 0$ and $\Delta f = f_n$. In the present analysis $\Delta f = 0.0051$ Hz.

The approximation described above is valid if the QTF changes slowly around the main diagonal corresponding to $\Delta f = 0$ (which is the same as saying the QTF is nearly constant along diagonals with constant $f_1 + f_2$). The assumption is in some sense similar, but not the same, to that of the Newman's approximation for the QTF off-diagonal terms (Newman, 1974).

Figure 8, further ahead in the text, with an empirical surge QTF shows that in fact the assumption referred in the previous paragraph may be questionable for the Exwave FPSO. One observes that the drift coefficients magnitude change around the main diagonal with $\Delta f = 0$. This may be particularly relevant for frequencies below around 0.08 Hz, where the QTF increases from small values for $\Delta f = 0$ to moderate values as Δf increases (before it reduces again). This aspect is discussed with more detail in the following Section.

The empirical coefficients are compared with potential flow predictions from MULDIF with zero current velocity. The following graphs present mean forces normalized by the wave amplitude squared as function of the wave frequency. Table 2 presents the seastate conditions for the selected test cases, together with an estimation of the seastate steepness, Sp:

$$S_p = \frac{2\pi}{g} \frac{H_S}{T_P^2} \qquad (1)$$

Figure 4 presents empirical wave drift coefficients for three moderate seastates, together with potential flow predictions (MULDIF). There is no current and the vessel heading is 0 degrees. MULDIF results represent mean wave drift coefficients in harmonic waves (difference frequency, $\Delta f = 0$), while the test results are extracted from the empirical QTF from a diagonal corresponding to $\Delta f = 0.0051$ Hz. The horizontal axis represents $(f_1+f_2)/2$, where f_1 and f_2 are the pair of frequency components.

There is a quite good agreement between the empirical and the potential flow coefficients for frequencies above around 0.075 Hz. It is plausible to assume the moderate seastates are within the range of applicability of the linear potential flow theory and that this is the reason why the agreement is good in this range. For frequencies lower than 0.075 Hz, the predictions reduce rapidly to zero, while the empirical coefficients are significantly larger. These differences are quite relevant since the severe seastates have great part of the energy within this frequency range. While it is still not possible to explain the discrepancies, there are indications that the exciting force QTF increases rapidly around the zero difference frequency diagonal for low frequencies (see Section 4.3).

This behaviour might explain the discrepancies, since the identification procedure assumes the QTF changes slowly around the main diagonal. The presented empirical coefficients correspond to an off-diagonal of the QTF, and not to the main diagonal. Section 4.3 discusses further this point.

Table 2: Test cases selected for analysis.

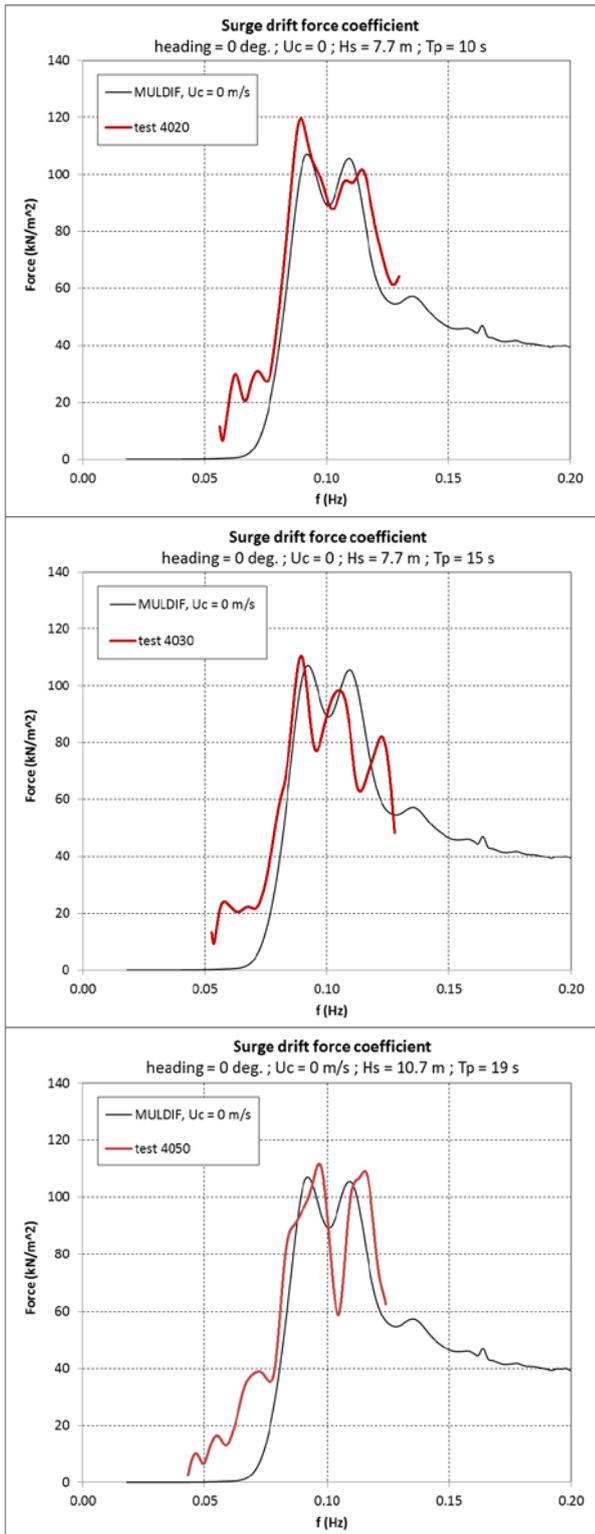| Test no.	Uc [m/s]	Hs [m]	Tp [s]	Head. [deg]	Sp [-]
4020	0.00	7.7	10	180	0.049
4030	0.00	7.7	15	180	0.022
4050	0.00	10.5	19	180	0.019
4130	0.97	7.7	15	180	0.022
4140	0.97	16.1	15	180	0.046
4160	0.97	21	19	180	0.037
4230	1.87	7.7	15	180	0.022
4071	0.00	3.5	6-30	160	-
4081	0.00	16.1	15	160	0.046

Figure 4: Surge wave drift force coefficients for three moderate sea states and Uc =0. MULDIF results for $\varDelta f = 0$ and empirical coefficients for $\varDelta f = 0.0051$ Hz.

Figure 5 shows the surge wave drift coefficients for head waves and three seastates with increasing significant wave height (Hs). The current velocity is 0.97 m/s and collinear with the waves. The empirical coefficients increase with the seastate severity, but not much.
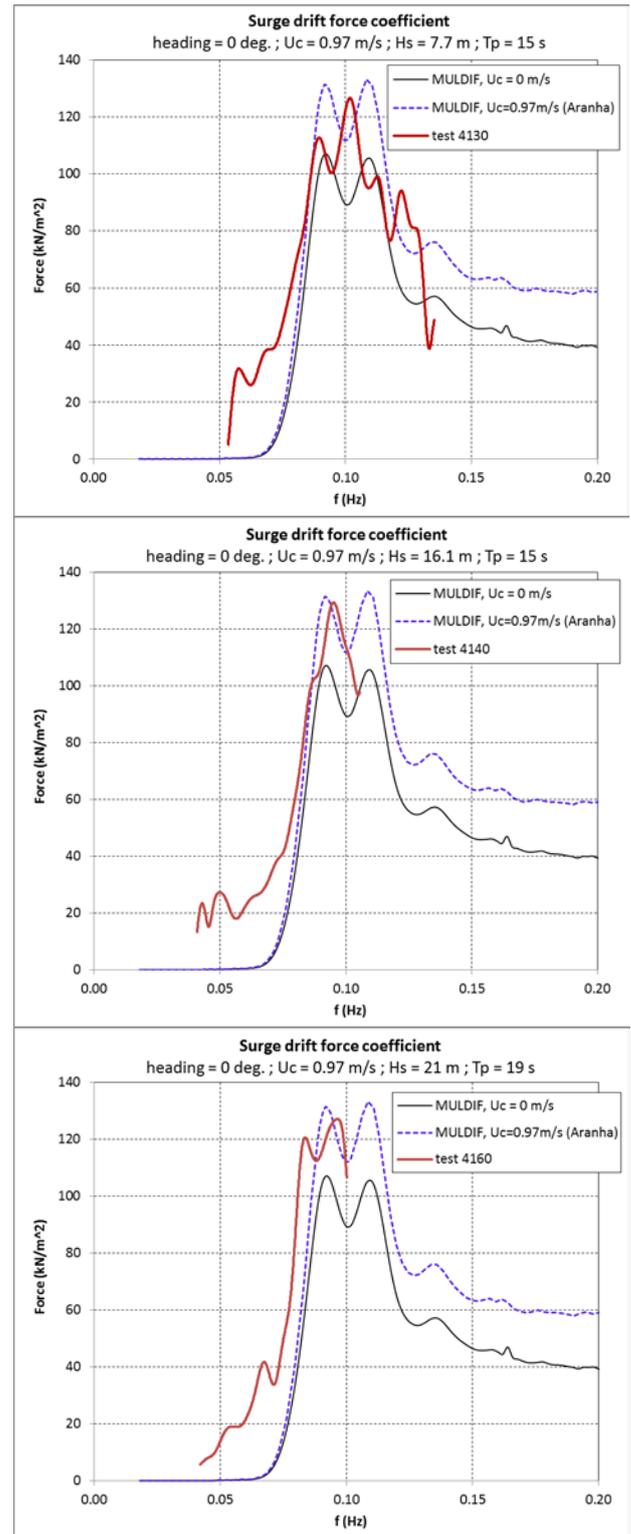
Figure 5: Surge wave drift force coefficients for three seastates with increasing Hs and Uc = 0.97 m/s. MULDIF results for $\varDelta f = 0$ and empirical coeffs. for $\Delta f = 0.0051$ Hz.

The wave-current interaction effects on surge wave drift forces is illustrated in Figure 6. The results correspond moderate seastates, with the same Hs and Tp and three different current velocities. The vessel heading is 0 degrees and waves and current are collinear. Results from tests are

5

compared with MULDIF, where the wave-current interaction effects were estimated by Aranha's (1994) formula. It is possible to observe that the wave drift forces increase with the current velocity. The simplified Aranha's formula captures reasonably well the drift forces curve peak increase with the current velocity, but differences are noted between 0.08 Hz and 0.09 Hz.

The identification method was also applied for bow waves (-20 degrees) with good results. Figure 7 presents the related sway drift force coefficients for a small and a large seastate and zero current. There is a good agreement between the empirical and the numerical drift coefficients for both seastates, which seems to indicate that nonlinear effects are not important for this case, except for frequencies below 0.075 Hz, where, again, the empirical results are larger than the predictions.

4.3 Full QTF estimates

Contour plots of full QTF estimates for selected tests are presented in Figure 8 for surge in test number 4030 as an example to highlight two essential items in this analysis as described below.

The green and pink dashed lines represent the QTF diagonal and the off-diagonal at difference frequency around Δf = 0.0051 Hz (pink line), respectively. The QTF modulus values extracted at the pink line represent the mean drift coefficients shown in Section 4.3. The reasons for choosing this line, instead of the real diagonal (main diagonal) are: 1) most of the signal energy is in this range, so resulting LF motions are dominated by it, and 2) measured values at the real diagonal are considered to be more contaminated by measuring errors.
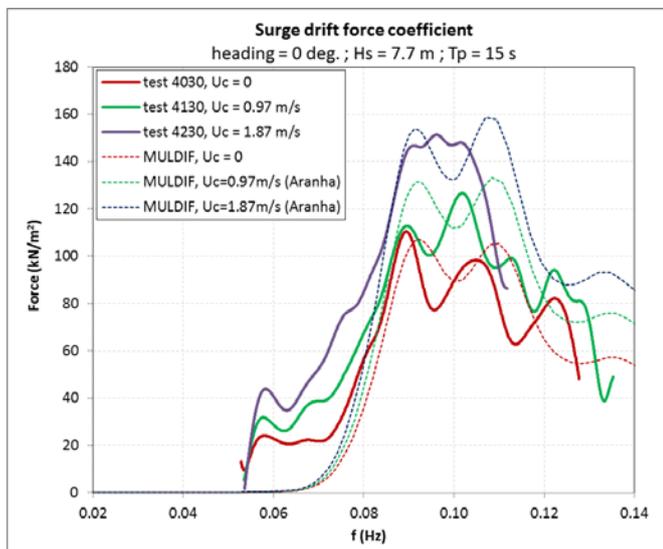

Figure 6: Comparison of surge wave drift force coeffs. for one moderate seastates and three current velocities. MULDIF results for Δf = 0 and empirical coeffs. for Δf = 0.0051 Hz.

Secondly, it can be observed that the QTF exhibits clear off-diagonal variations in the Δf-range up to the natural frequency of the moored floater motion, in both modulus and phase. In particular, for long waves with f < 0.08 Hz (T > 12 s), where most of the wave energy is located in design sea

states, the QTF increases with increasing Δf. Hence, the use of Newman's approximation, which assumes that the off-diagonal variation is small in the actual Δf-range, will be non-conservative for the present case.
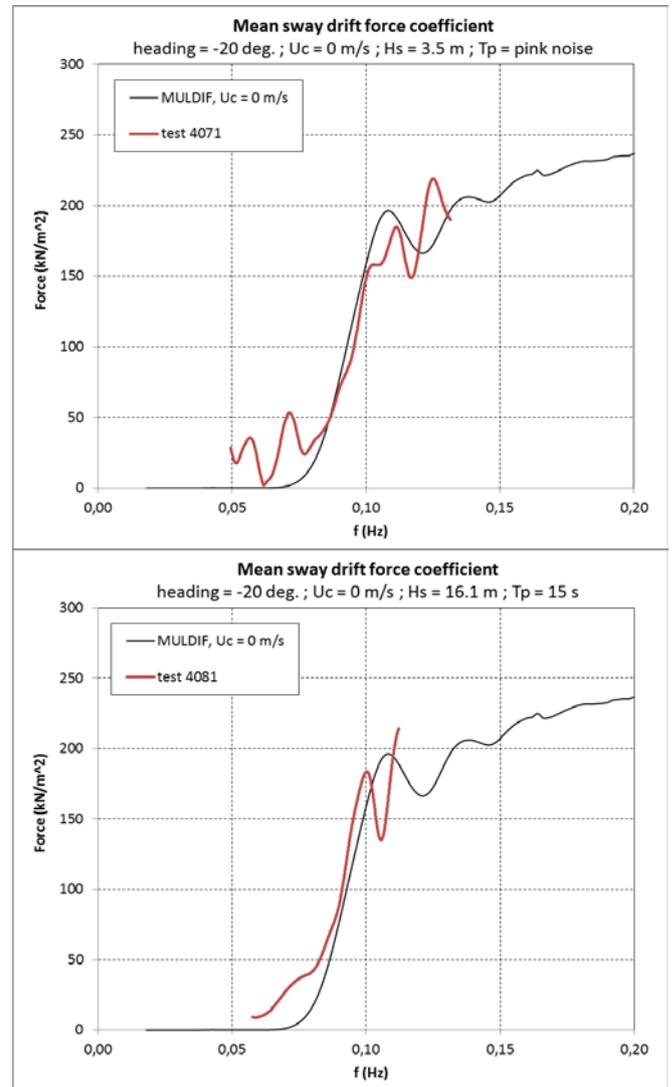

Figure 7: Comparison of sway wave drift coefficients for two seastates. Vessel head. = -20 deg., Uc = 0. MULDIF results for Δf = 0 and empirical coeffs. for Δf = 0.0038 Hz.

The fact that Newman's approximation seems un-conservative for this case study is somewhat surprising, since it is usually assumed to work well for deep water conditions and LF motions with long natural periods. In this case, the surge natural period is 169.6 s. On the other hand, it is well known that the effect described above is present in shallow water.

The referred off-diagonal increase explains the deviation from MULDIF drift coefficients observed for long waves in Figure 4 of Section 4.2, as well as in the other plots in the same Section, since we extract the coefficients from the pink line. The lower plot of Figure 8 shows the phase increases rapidly with Δf and roughly approaches 90 degrees for low frequencies. This is an indication that the off-diagonal increase of the modulus is due to an increase in the imaginary part of the QTF, i.e. in the second-order potential.
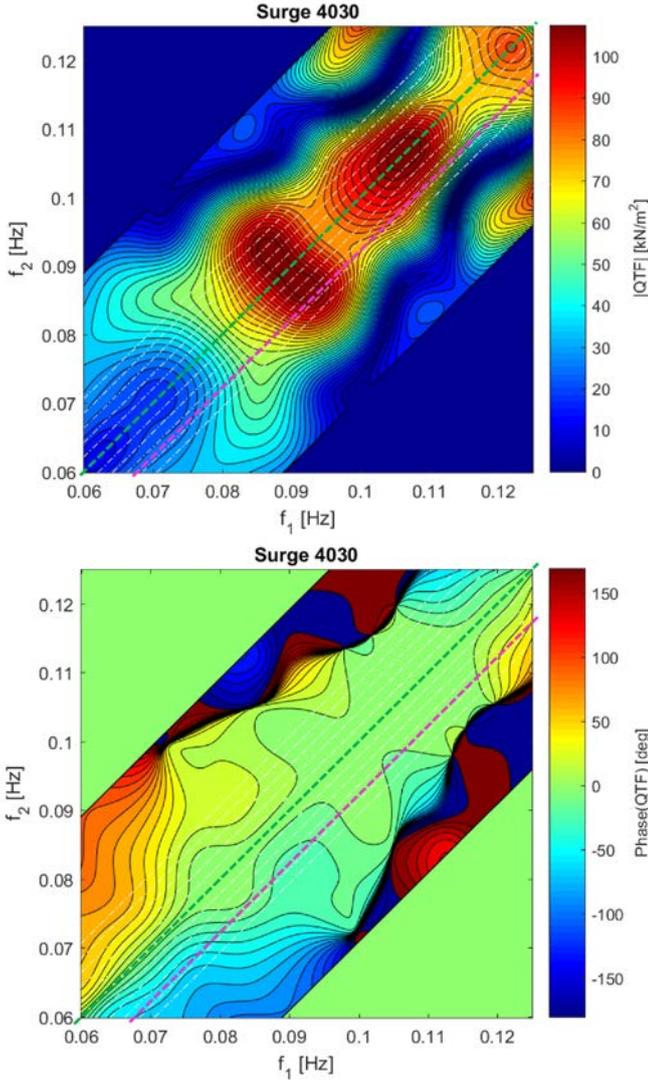
Figure 8: Surge force full QTF estimate contour plot example. Hs=7.7m, Tp=15s, head. = 0 deg., Uc=0. Upper graph: modulus; Lower graph: phase.

Analysis of QTFs from additional test cases show a similar trend as that of Figure 8, with an off-diagonal QTF variation in the actual Δf-range. We notice in particular the general trend for wave frequencies lower than about 0.08Hz, where the QTF increases with Δf. This is observed for moderate as well as high sea states, and with current as well as without. For the high sea states with current, the QTF magnitudes are generally higher.

More detailed studies are needed to clarify the behaviour of the difference frequency wave drift force full QTF and verify if other FPSOs hulls shows similar trends as those identified for the Exwave FPSO. It is also important to check the consequences of applying Newman's approximation in this case, since such approximation is usually assumed valid for deepwater conditions and motions with long natural periods.

5   SLOW DRIFT DAMPING

As described in Section 3.1, the wave drift force coefficients estimation from irregular wave tests includes two major steps:
- First, the low frequency (LF) wave exciting force is estimated from the measured LF motion assuming the latter is represented by a linear mass-damper-spring system.
- Second, a cross bi-spectral analysis is applied to the wave elevation and the estimated response (excitation) to achieve the QTF.

Besides the excitation, the first step involves one additional unknown, namely the LF damping. For this reason, the QTF estimation follows an iterative process where the damping is systematically adjusted until a good convergence of the measured and reconstructed LF motion spectra is achieved. A linearized form of the LF damping is a result of the identification procedure. The present Section discusses these results.

The horizontal mooring linear stiffness is taken from the load excursion curve as identified from pull out tests (Figure 9). The surge restoring coefficient is:

$$K = 268 \ kN/\text{m} \qquad (2)$$

One additional piece of information useful for the present analysis is the linear and quadratic damping coefficients identified from the decay tests. Figure 10 presents the surge relative damping as function of the mean motion amplitude from a decay tests without current. It is possible to observe that the LF damping is nearly quadratic, since the relative damping increases almost linearly with the motion amplitude. There is also a small linear damping contribution Table 2 shows system parameters identified from the decay tests with Uc = 0 and 0.97 m/s, namely the surge natural periods, the linear damping coefficients (B^L) and the quadratic damping coefficients (B^Q). The surge total mass applied for the following analysis is:

$$m = 1.9254E + 08 \ \text{Kg} \qquad (3)$$

where the MULDIF zero current added mass was applied for conditions both with and without current.

The calm water linear and quadratic damping coefficients were applied to estimate an equivalent linearized damping, B^*. The surge low frequency damping forces by the linearized and by the quadratic models are given respectively by:

$$F_d^L = B^* \dot{x}_{LF}(t) \qquad (4)$$

$$F_d^Q = B^L \dot{x}_{LF}(t) + B^Q \dot{x}_{LF}(t)|\dot{x}_{LF}(t)| \qquad (5)$$

where $\dot{x}_{LF}(t)$ is the surge low frequency velocity.

Assuming the dissipation of energy, related to the damping forces, by the linearized and the quadratic models are the same, the linearized damping may be estimated as:

$$B^* = \frac{\int_0^T [B^L \dot{x}_{LF}(t) + B^Q \dot{x}_{LF}(t)|\dot{x}_{LF}(t)|] \dot{x}_{LF}(t) dt}{\int_0^T \dot{x}_{LF}(t) \dot{x}_{LF}(t) dt} \qquad (6)$$

Equation (6) provides an estimation of the surge low frequency linearized damping in waves, if the linear and quadratic damping coefficients in calm water would remain

7

unchanged for LF motions in waves. B^* was estimated for several of the tested cases applying (6) together with the measured $\dot{x}_{LF}(t)$.
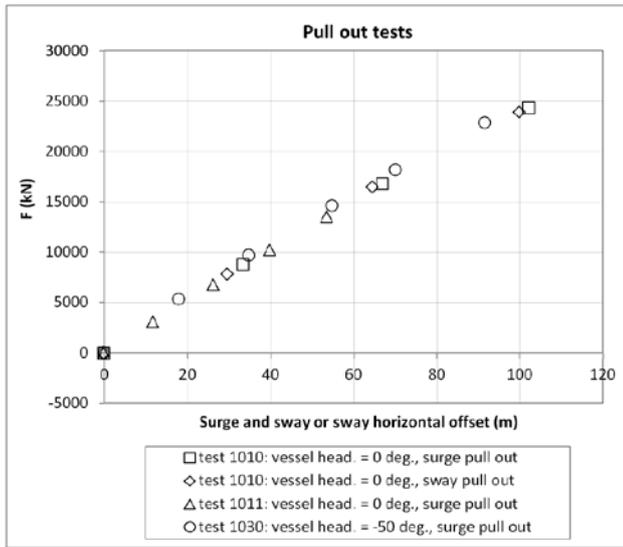

Figure 9: Exwave FPSO mooring system horizontal restoring force from pull out tests
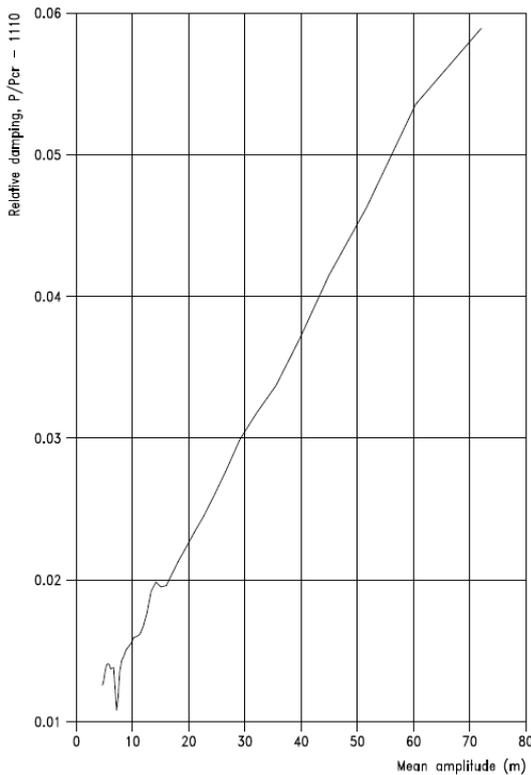

Figure 10: Surge relative damping (damp. factor) with Uc = 0

Finally, Table 3 presents the LF system parameters identified from several of the tests in waves:
- Columns number four and five show the mean surge offset and the LF surge standard deviation in waves.
- Column number six presents the surge natural period adjusted to achieve a good agreement between the measured and reconstructed LF surge spectra peaks.

- Column number seven includes the surge relative damping (Rel. damp.) estimated from the cross bi-spectral (CBS) analysis procedure. This may be regarded as the actual linearized damping in waves (relative damping represents the actual damping normalized by the critical damping).
- Column number eight presents the surge relative damping from formula (6). This is the linearized damping in case the damping coefficients in waves would be the same as identified from the calm water tests (decay tests).

Table 2: Surge natural period estimated from the decay tests

Decay mode	Uc [m/s]	Decay Tn [s]	B^L/m [1/s]	B^Q/m [1/m]
Surge	0.00	169.6	6.472E-04	1.683E-03
Surge	0.97	168.0	3.165E-03	2.012E-04

Table 3: Surge low frequency system parameters

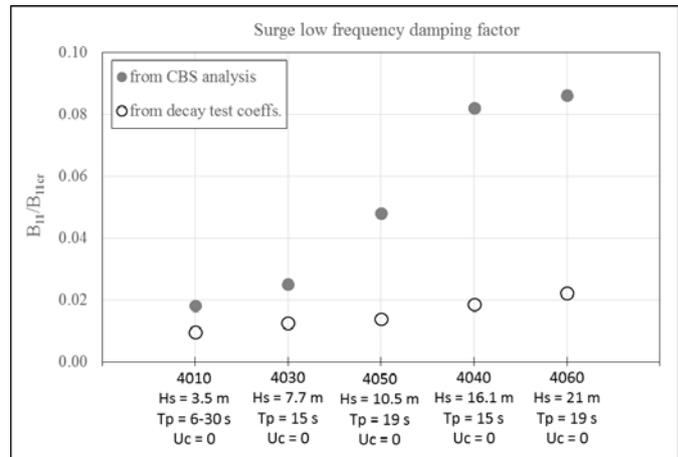| Test no.	Hs [m]	Tp [s]	Mean offset [m]	Stdv [m]	Tn [s]	Rel. damp. CBS [%]	Rel. damp. decay coeffs. [%]
4010	3.5	pink	-0.36	0.65	169	1.8	1.0
4030	7.7	15	-1.23	2.76	168	2.5	1.3
4050	10.5	19	-1.69	3.66	164	4.8	1.4
4040	16.1	15	-4.92	7.18	163	8.2	1.8
4060	21.0	19	-5.19	9.03	171	8.6	2.2

Figure 11: Surge low frequency damping factor estimated for different seastates.

The linearized damping of the actual LF motion (8th column) is very small for the low seastate and it increases significantly for severe seastates, which would be expected since the damping is of quadratic nature and the LF amplitudes (and velocities) increase with the seastate (see the standard deviations).

One observes an increase of the actual damping, compared to the predictions by the calm water damping model (Figure 11). In Figure 11, the full circles represent the actual linearized damping in waves identified by the cross bi-spectral analysis procedure, while the open circles represent the damping estimated by equation (6). The latter is the damping that would be present if the linear and quadratic damping identified from the decay test would represent the damping in waves. The difference represents the damping

8

increase due to wave effects – the damping in waves is larger than in calm water. The increase is partly related to slow drift damping effects (modification of the drift forces due to slow drift velocities). Probably, there is also a contribution related to additional viscous effects due to wave frequency relative motions between the vessel and the waves. The increase is significant for severe seastates.

It is important to note that a significant contribution to the LF surge damping arises from the horizontal mooring system. This aspect requires further analysis.

6   CONCLUSIONS

The paper presents and discusses horizontal wave drift force coefficients and low frequency damping coefficients for the Exwave FPSO under moderate and severe seastates. Model test data is used to identify the coefficients.

A second order signal analysis technique is applied to identify the difference frequency wave exciting QTF. Good agreement between the measured and reconstructed low frequency (LF) motions validates the procedure.

Comparison of wave drift coefficients extracted from a diagonal with difference frequency (Δf) close to the system natural frequency, from different test cases with Uc = 0, shows the empirical drift coefficients increase with the seastate severity, but not much. Collinear wave-current interaction effects increase further the drift forces.

Zero Δf potential flow predictions underestimate the empirical drift coefficients from Δf diagonals near the system natural frequency. The underestimation is visible for frequencies below 0.075 Hz. The observation contradicts the usual assumption that the QTF changes slowly around the main diagonal for deep water systems with long natural periods. In fact, the empirical QTFs show off-diagonal variations in the Δf-range up to the natural frequency of the moored floater motion. This is important in particular for numerical simulation methods making use of Newman's approximation. But also for other methods where off-diagonal variation is in fact taken into account, the present results will be useful for detailed comparison studies in future work.

Compared to the calm water damping, the surge low frequency damping increases significantly with the seastate severity.

7   ACKNOWLEDGEMENTS

8   REFERENCES

Aksnes, V.Ø., 2014. "Correct" response in positioning analyses. Tekna Conference on DP and Mooring of Floating Structures Offshore, Trondheim, Norway, 12-13 February 2014.

Aksnes, V.Ø, Berthelsen, P., Fonseca, N., and Reinholdtsen, S.-A., 2015. On the need for calibration of numerical models of large floating units against experimental data. Proceedings of the 25th International Ocean and Polar Engineering Conference, June 21-26, Kona, Hawaii, USA.

Aranha, J. A. P., 1994. A Formula for Wave Damping in the Drift of Floating Bodies. Journal of Fluid Mechanics, Vol. 275, pp. 147–155.

DNV, 2010. Environmental conditions and environmental loads. Recommended practice DNV-RP-205, October 2010.

Fonseca, N., Stansberg, C.T., Nestegård, Bøckmann, A., Baarholm, R., 2016. The EXWAVE JIP: Improved procedures to calculate slowly varying wave drift forces on floating units in extreme seas. Proc. of the ASME 2016 35th Int. Conf. on Ocean, Offshore and Arctic Eng., June 19-24, 2016, Busan, South Korea, paper OMAE2016-54829.

Fonseca, N. and Stansberg, C.T., 2017. Wave drift forces and low frequency damping on the Exwave Semi-submersible. Proc. of the ASME 2017 36th Int. Conf. on Ocean, Offshore and Arctic Eng., June 25-30, 2017, Trondheim, Norway, paper OMAE2017-62540.

Fonseca, N., Ommani, B., Stansberg, C.T., Bøckmann, A., Birknes-Berg, J., Nestegård, A., de Hauteclocque, G., Baarholm, R., 2017. Wave Forces and Low Frequency Drift Motions in Extreme Seas: Benchmark Studies. Proceedings of the Offshore Technology Conference, paper OTC-27803-MS, 1-4 May 2017, Houston, TX, USA.

Hermundstad, E.M., Hoff, J.R., Stansberg, C.T. and Baarholm, 2016. Effects of wave-current interaction on floating bodies. Proc. of the ASME 2016 35th Int. Conf. on Ocean, Offshore and Arctic Eng., June 19-24, 2016, Busan, South Korea, paper OMAE2016-54868.

Newman N., 1974. Second-order, slowly-varying forces on vessels in irregular waves. Proc. Symp. on the Dynamics of Marine Vehicles and Structures in Waves, London, UK, 182-186, April 1974.

Pakozdi, C., 2014. QTF code verification. MARINTEK report no. 580279-01.

Stansberg, C.T., 1997. Linear and nonlinear system identification in model testing. International Conference on Nonlinear Aspects of Physical Model Tests, OTRC, Texas A&M University, College Station, Texas, 2-3 May 1997.

Stansberg, C.T. 2001. Data Interpretation and System Identification in Hydrodynamic Model Testing. Proc of 11th Int. Offshore and Polar Eng. Conf., ISOPE, Stavanger, Norway.

Stansberg, C.T. and Pakozdi, C., 2009. Slowly varying wave drift forces analysed from model test data on a moored ship in shallow water. Proceedings of the ASME 2009 28th International Conference on Ocean, Offshore and Arctic Engineering, OMAE2009, May 31 – June 5, Hawaii, Honolulu, paper OMAE2009-79491.

Stansberg, C.T., Kaasen, K.E., Abrahamsen, B.C., Nestgård, A., Shao, Y., Larsen, K., 2015. Challenges in Wave Force Modelling for Mooring Design in High Seas. Proceedings of the Offshore Technology Conference, paper OTC-25944-MS, 4-7 May 2015, Houston, TX, USA.